JACS
JOURNAL OF THE AMERICAN CHEMICAL SOCIETY
Article
pubs.acs.org/JACS

Gating That Suppresses Charge Recombination—The Role of Mono-*N*-Arylated Diketopyrrolopyrrole

Anna Purc,[†] Eli M. Espinoza,[‡] Rashid Nazir,[†] Juan J. Romero,[§] Kamil Skonieczny,[†,§] Artur Jeżewski,[†] Jillian M. Larsen,[§] Daniel T. Gryko,*[,†] and Valentine I. Vullev*[,‡,§]

[†]Institute of Organic Chemistry, Polish Academy of Sciences, Kasprzaka 44-52, 01-224 Warsaw, Poland
[‡]Department of Chemistry and [§]Department of Bioengineering, University of California, Riverside, California 92521, United States

Supporting Information

ABSTRACT: Suppressing the charge recombination (CR) that follows an efficient charge separation (CS) is of key importance for energy, electronics, and photonics applications. We focus on the role of dynamic gating for impeding CR in a molecular rotor, comprising an electron donor and acceptor directly linked via a single bond. The media viscosity has an unusual dual effect on the dynamics of CS and CR in this dyad. For solvents with intermediate viscosity, CR is 1.5−3 times slower than CS. Lowering the viscosity below ∼0.6 mPa s or increasing it above ∼10 mPa s makes CR 10−30 times slower than CS. Ring rotation around the donor−acceptor bond can account only for the trends observed for nonviscous solvents. Media viscosity, however, affects not only torsional but also vibrational modes. Suppressing predominantly slow vibrational modes by viscous solvents can impact the rates of CS and CR to a different extent. That is, an increase in the viscosity can plausibly suppress modes that are involved in the transition from the charge-transfer (CT) to the ground state, i.e., CR, but at the same time are not important for the transition from the locally excited to the CT state, i.e., CS. These results provide a unique example of synergy between torsional and vibronic modes and their drastic effects on charge-transfer dynamics, thus setting paradigms for controlling CS and CR.

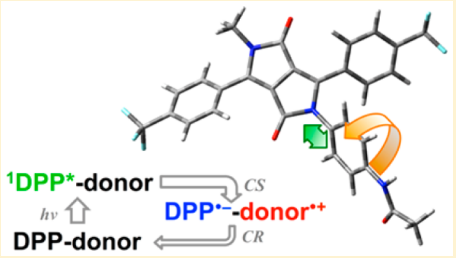

INTRODUCTION

Controlling electron transfer (ET) at a molecular and nanoscale level is paramount for improving the performance of energy-conversion materials and devices. Suppressing charge recombination (CR) that follows photoinduced charge separation (CS) renders solar energy conversion-efficient. Local fields originating from molecular electric dipoles, anisotropic covalency, and cascade ET events, bypassing localized charge-transfer (CT) states and changes in multiplicity, provide an invaluable means for suppressing undesired CR.[1−6]

Optimizing CS driving force, $-\Delta G_{CS}^{(0)}$, and reorganization energy, λ, to attain activationless CS ($-\Delta G_{CS}^{(0)} \approx \lambda$) can impede CR by placing it in the Marcus inverted region ($-\Delta G_{CS}^{(0)} > \lambda$).[7−9] This nonadiabatic semiclassical view focuses on the Franck−Condon aspects of ET.

Conformational gating, which is important for biology, presents another approach for controlling ET.[10] By impacting the electronic coupling along the ET pathways, non-Condon effects from torsional dynamics can define the CT properties of molecular systems.[11,12] The utility of such effects for energy materials and organic electronics cannot be overstated.

With structural features resembling those of indigo and with superior thermal stability and light-fastness, diketopyrrolopyrrole (DPP) derivatives are organic dyes with promising properties for optoelectronics.[13] Due to their strong light absorption, high fluorescence quantum yields and reduction potentials making them relatively good electron donors and acceptors, DPPs have undergone significant repositioning from high-quality pigments[14] to organic electronic materials[15,16] toward dyes for fluorescence-based applications.[17−21]

To explore the effects of gating on single-step CS and CR processes, herein we focus on the ET properties of an electron-deficient diketopyrrolopyrrole (**DPP**, Figure 1a) that we derivatize with moderately good electron donors. While **DPP** is strongly fluorescent, the emission of **DPP-Ph** with the donor, 4-acylaminophenyl, directly linked to one of the lactam nitrogens (Figure 1a), is considerably quenched (Figure 1b). This is fluorescence loss due to highly efficient intramolecular CS that the photoexcited **DPP-Ph** undergoes to produce a non-fluorescent CT state. As expected, the rate constants of CS and CR, k_{CS} and k_{CR}, respectively, manifest correlations with the media polarity. An important characteristic for efficient conversion of the harvested light energy is k_{CS}/k_{CR}, representing how much slower CR is in comparison with CS. The polarity and proticity of the solvent do not appear to correlate with k_{CS}/k_{CR}. Conversely, k_{CS}/k_{CR} exhibits a defined bimodal correlation with the media viscosity. That is, k_{CS}/k_{CR} is largest for the most and the least viscous solvents, regardless their polarity or proticity.

RESULTS AND DISCUSSION

Synthetic Strategies. The synthesis of the CT conjugates requires the preparation of asymmetrically substituted DPP derivatives. While the synthesis and double *N*-alkylation of

Received: May 14, 2016
Published: September 12, 2016

DOI: 10.1021/jacs.6b04974
J. Am. Chem. Soc. 2016, 138, 12826−12832

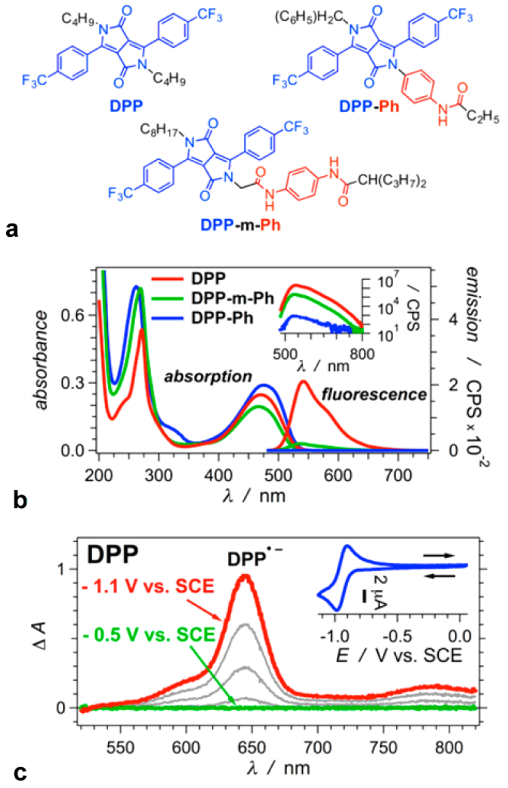

Figure 1. Basic characteristics of **DPP**, **DPP-Ph**, and **DPP-m-Ph**. (a) Structures. (b) UV/visible absorption and fluorescence spectra (10 μM in acetonitrile, MeCN). Inset: fluorescence spectra plotted against logarithmic ordinate (λ_{ex} = 470 nm, fluorescence quantum yields $\phi_f^{(DPP)}$ = 0.75, $\phi_f^{(DPP\text{-}m\text{-}Ph)}$ = 0.073, $\phi_f^{(DPP\text{-}Ph)}$ = 3.6 × 10^{-4}). (c) Differential absorption spectra recorded during electrochemical reduction of **DPP** (for MeCN with 100 mM NBu_4PF_6). Inset: cyclic voltammogram of **DPP** (scan rate =50 mV s^{-1}).

these pigments is easy and well-established,[13] the *N*-arylation is extremely challenging; currently, we know of only two reported cases that utilize strongly activated aryl fluorides.[22] Our design requires full control over the pattern of substituents. Therefore, we adopted a general strategy reported by Morton et al.[23−25]

The selected route is based on the synthesis of the targeted furo[3,4-*c*]pyrrole, **5**, followed by a sequence of alkylation and amidation steps (Scheme 1). Initial alkylation of β-keto ester, **1**, with ethyl bromoacetate in the presence of a strong base affords **2** in a good yield. Ammonia-induced ring closure results in the dihydropyrrolone, **3**, with one of the electron-deficient aryl substituents attached to it. A somewhat challenging alkenylation of the methylene carbon, followed by microwave-induced ring closure yields **5**. Alkyl bromides, regardless the use of different bases (K_2CO_3, Cs_2CO_3, *t*-BuOK, and NaH), solvents (DMF, NMP, and THF), catalysts (TBAHS, KI, and crown ethers), and ultrasonication, manifest limited reactivity with **5**. Therefore, we resort to benzyl bromide as a more active alkylation agent, affording *N*-benzylfuro[3,4-*c*]pyrrole **6** in 27% yield. Asymmetrically *N*,*N*-disubstituted **DPP**, obtained via amidation from **6**, is readily acylated to the final compound, **DPP-Ph**, with excellent yield (Scheme 1).

The other CT conjugate, **DPP-m-Ph**, possesses the same electron-deficient chromophore, but a methylene links it with the donor (Figure 1a). For the synthesis of this asymmetric conjugate, we use statistical *N*,*N*-dialkylation of a symmetric DPP derivative, **7** (Scheme 2).

Basic Photophysical Properties. **DPP** exhibits visible absorption and fluorescence, with zero-to-zero energy, $\mathcal{E}_{00}$, of about 2.4 eV. Addition of the electron donors does not cause substantial wavelength shifts in the absorption and emission spectra, but does considerably quench the fluorescence (Figure 1b). The absorption maxima for **DPP**, **DPP-Ph**, and **DPP-m-Ph** are at 470, 476, and 467 nm. Because $\Delta G_{CS}^{(0)}$ vales for **DPP-Ph** and **DPP-m-Ph** are around −0.2 eV for acetonitrile media (Table 1), the 6 nm bathochromic shift in the absorption of **DPP-Ph** (corresponding to 33 meV) cannot be unequivocally ascribed to a CT band. These results suggest that while the DPP-donor dyads undergo highly efficient CS the donor−acceptor electronic coupling in these conjugates is not strong enough to considerably perturb the DPP absorption.

While this finding is not surprising for methylene-linked donor−acceptor systems[1,34] such as **DPP-m-Ph**, it is unusual for **DPP-Ph**. CT conjugates, in which the donor and the acceptor are linked with a single bond, tend to exhibit defined bathochromic CT absorption.[35,36] In **DPP-Ph**, however, the link is via a lactam nitrogen, which is spatially near some of the nodes of the frontier orbitals.[37,38] Indeed, the C−C bonds anchoring the trifluoromethylphenyl moieties to the principal DPP ring system at positions 3 and 6 provide strong π-electronic coupling. Therefore, the trifluoromethyl groups affect the whole chromophore, making it electron-deficient. Conversely, groups attached to the lactam nitrogens do not truly perturb the DPP

Scheme 1. Synthesis of Asymmetrically Arylated Diketopyrrolopyrrole DPP-Ph[a]

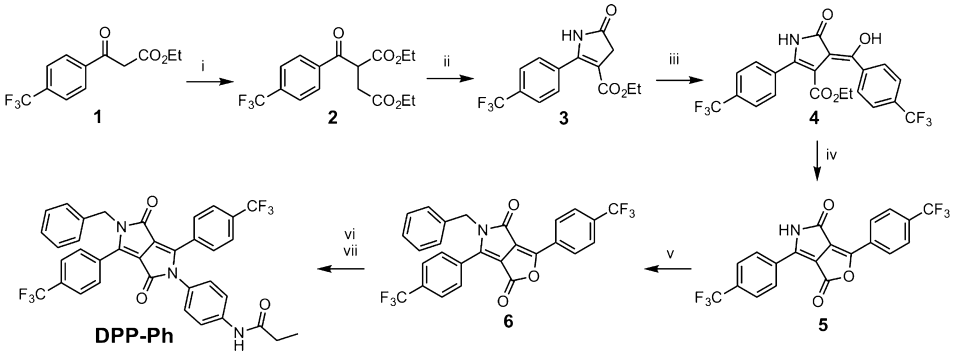

[a](i) $BrCH_2CO_2Et$, EtONa, EtOH, 0 °C → rt, 89%; (ii) NH_4OAc, AcOH, reflux, 63%; (iii) 1-CF_3-$C_6H_4CO_2Et$, *t*-AmONa, *t*-AmOH, 60 °C, 23%; (iv) microwave, 230 °C, 10 min, 74%; (v) $C_6H_5CH_2Br$, K_2CO_3, DMF, 40 °C, 29%; (vi) 1,4-$(NH_2)_2C_6H_4$, EDC, TFA, DCM, rt, 59%; and (vii) $(CH_3CH_2CO)_2O$, NEt_3, DCM, 0 °C → rt, 99%.

DOI: 10.1021/jacs.6b04974
J. Am. Chem. Soc. 2016, 138, 12826−12832

Scheme 2. Synthesis of Asymmetrically Alkylated Diketopyrrolopyrrole DPP-m-Ph[a]

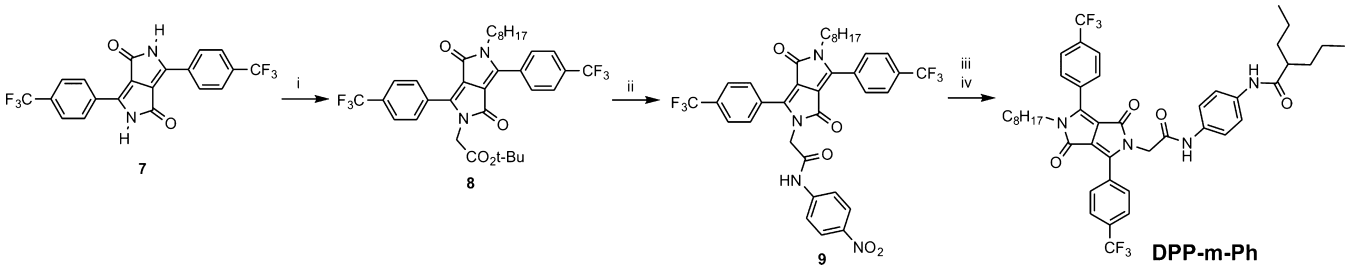

[a](i) $BrCH_2CO_2$-*t*-Bu, $C_8H_{17}I$, Cs_2CO_3, NMP, 120 °C, 25%; (ii) 1. TFA, DCM, 0 °C → rt; 2. $(COCl)_2$, DCM, rt, 1 h, 3. *p*-nitroaniline, pyridine, DCM, rt, 1 h, overall 84%; (iii) $Co_2(CO)_8$, H_2O, DME, reflux, 1 h, 67%; and (iv) $(H_7C_3)_2CHCOCl$, pyridine, rt, 1 h, 89%.

Table 1. Estimates for CS Driving Forces, $-\Delta G_{CS}^{(0)}$

			$E^{(1/2)}$ (V vs SCE)[b]		
		$\mathcal{E}_{00}$ (eV)[a]	$D^{\bullet+}/D$	$A/A^{\bullet-}$	$\Delta G_{CS}^{(0)}$ (eV)[c]
DPP-Ph	MeCN	2.42	1.39	−0.89	−0.21
	DCM	2.39	1.54	−0.87	−0.29
DPP-m-Ph	MeCN	2.43	1.32	−0.90	−0.25
	DCM	2.42	1.55	−0.84	−0.23

[a]The values of the zero-to-zero energy, $\mathcal{E}_{00}$, were obtained from the wavelengths, λ_{00}, of the crossing points of the normalized absorption and fluorescence spectra: i.e., $\mathcal{E}_{00} = hc/\lambda_{00}$.[26,27] [b]Values of half-wave potentials, $E^{(1/2)}$, extrapolated to zero electrolyte concentration, representing the reduction potentials for neat solvents.[28−32] $E^{(1/2)}$ for $D^{\bullet+}/D$ was obtained from the first oxidation waves of the cyclic voltammograms of the dyads, and for $A/A^{\bullet-}$, it was obtained from the first reduction waves. [c]Calculated from eq 1, where $\Delta G_S = 0$ and $W = e^2/4\pi\varepsilon_0\varepsilon R_{DA}$:[33] e, electron charge, ε, static dielectric constant of the solvent (Table 2), $\varepsilon_0 = 5.526 \times 10^{-3}$ e V^{-1} $Å^{-1}$, and R_{DA} the donor−acceptor center-to-center distances, was ∼5.2 Å for **DPP-Ph** and 7.2 Å for **DPP-m-Ph**.

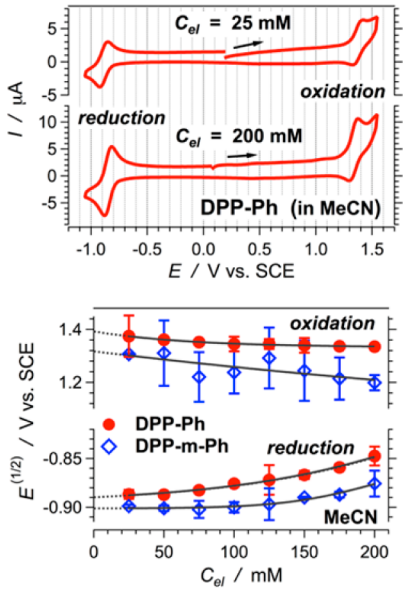

Figure 2. Electrochemical oxidation and reduction of **DPP-Ph** and **DPP-m-Ph**. (a) Cyclic voltammograms of **DPP-Ph** for MeCN at different concentrations, C_{el}, of supporting electrolyte, NBu_4PF_6. (b) Dependence of the half-wave reduction potentials on electrolyte concentration for MeCN. The solid lines are the data fits, and the dotted lines show the extrapolations to zero electrolyte concentration.

electronic properties as evident from the spectroscopic and electrochemical results.

Thermodynamics of Charge Separation. The Rehm−Weller equation provides a means for estimating the driving force, $-\Delta G_{CS}^{(0)}$, of photoinduced CS (Table 1):[28,39]

$$\Delta G_{CS}^{(0)} = F(E_{D^{\bullet+}/D}^{(0)} - E_{A/A^{\bullet-}}^{(0)}) - \mathcal{E}_{00} + \Delta G_S + W \qquad (1)$$

Electrochemically estimated half-wave reduction potentials, $E^{(1/2)}$, provide a good approximation for $E^{(0)}$ of the oxidation of the donor, D, and the reduction of the acceptor, A.[28] For solvents in which $\mathcal{E}_{00}$ is estimated from spectral data, we extrapolate $E^{(1/2)}$ to zero electrolyte concentration.[30,31,40] Thus, we eliminate the Born solvation term, ΔG_S, which corrects for the interactions of the formed radical ions with the solvent environment.[1,28] The Coulomb work term, W, accounts for the interactions between the generated radical ions.

We obtain $E_{D^{\bullet+}/D}^{(1/2)}$ and $E_{A/A^{\bullet-}}^{(1/2)}$ from the first oxidation and the first reduction waves, respectfully, in the cyclic voltammograms of **DPP-Ph** and **DPP-m-Ph** (Figure 2a). Extrapolation of the half-wave potentials to zero salt concentration allows for elimination of the effect of the supporting electrolyte (Figure 2b).[30−32] The close similarity between the reduction potentials of **DPP-Ph** and **DPP-m-Ph** (Table 1) suggests that the electron donors in the two dyads have (1) the same susceptibility to oxidation and (2) no effect on the reduction of DPP.

Employing these estimates for $E^{(1/2)}$ in eq 1 and factoring W yields similar CS driving forces for the two dyads (Table 1). In addition, the CS driving forces for the relatively polar acetonitrile (MeCN) appear slightly less favorable (with 50−80 meV) than those for the relatively nonpolar dichloromethane (DCM). Because the values of $-\Delta G_{CS}^{(0)}$ are relatively small, the Coulomb term, W (eq 1), has a major contribution to the estimates. The values of W, however, could be underestimates, especially for polar solvents. Typically, the calculations of W assume spherical radical ions of the oxidized donor and the reduced acceptor separated by a continuum media characterized with the dielectric constant, ε, of the bulk solvent. For linked donor−acceptor systems, the donor and the acceptor are in the same solvation cavity, and the space between them cannot be necessarily characterized with ε of the bulk media.[41] Therefore, the small differences between the calculated values for the CS driving forces are within the uncertainty of the W estimates, and $-\Delta G_{CS}^{(0)}$ should be larger, especially for MeCN.

Kinetics of Electron Transfer. Upon illumination, **DPP-Ph** forms a locally excited state, ^{1}**DPP*-Ph**, manifesting a broad transient absorption (Figure 3a,b). The picosecond decay of ^{1}**DPP*** is concurrent with the rise of a band at 640 nm, which corresponds to the reduced chromophore, **DPP**$^{\bullet-}$ (Figure 1c, 3b).

DOI: 10.1021/jacs.6b04974
J. Am. Chem. Soc. 2016, 138, 12826−12832

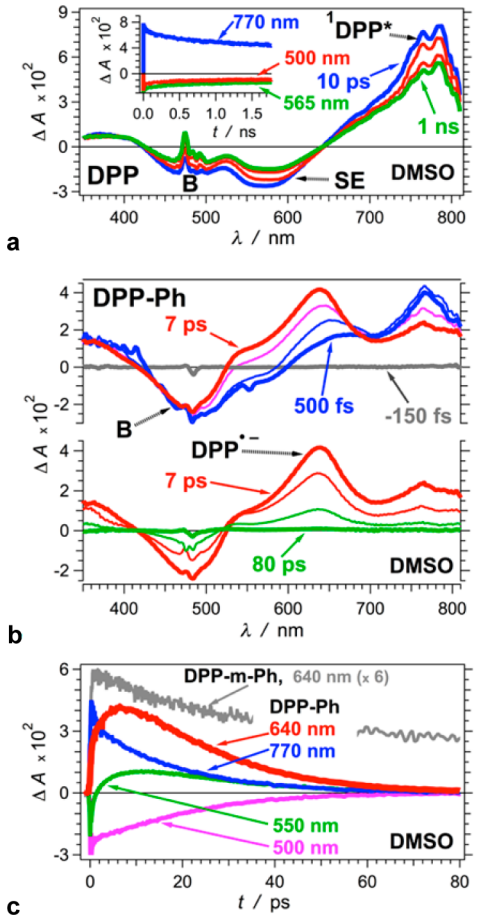

Figure 3. Transient absorption (TA) dynamics of **DPP** and **DPP-Ph** for DMSO (λ_{ex} = 480 nm, 6 μJ per pulse, fwhm$_{(for\ 800\ nm)}$ = 50 fs). (a and b) TA spectra (SE = stimulated emission, B = ground-state bleach). (c) TA dynamics monitored at different wavelengths: 770 nm for ^{1}**DPP***, 640 nm for **DPP**$^{\bullet-}$, 550 nm for SE, and 500 nm for B. For comparison, the top gray line is for **DPP-m-Ph** monitored at 640 nm (Figure 5b). The rest of the kinetic curves are for **DPP-Ph**.

DPP$^{\bullet-}$ decays simultaneously with the recovery of the ground state, as monitored at the bleach (Figure 3c). Therefore, we determine k_{CS} from the rise of the 640 nm band and k_{CR} from its decay, as quantified using global analysis.

A decrease in the media polarity tends to slow down both, CS and CR, which can be expected (Table 2).[1,33] This polarity dependence of k_{CS} and k_{CR} appears more pronounced for protic than for aprotic solvents; the correlations are stronger for CS than for CR (Figure 4a,b). These observations underline the effects of discrete solvent−solute interactions, such as hydrogen bonding, on the ET properties of **DPP-Ph** and especially on the initial photoinduced CS.

Conversely, the ratio k_{CS}/k_{CR} shows no apparent correlation with the solvent polarity. For protic and aprotic media, the correlations between k_{CS}/k_{CR} and the different representations of polarity are negligibly weak, i.e., $R^2 < 0.1$ (Figure 4c). A close examination of the k_{CS}/k_{CR} versus f_O plots, however, reveals two separate trends (Figure 4c): (1) For solvents more polar than EtOH, k_{CS}/k_{CR} tends to increase with polarity (R^2 ($\log(k_{CS}/k_{CR})$ vs $f_O(\varepsilon)$) = 0.47). (2) For solvent less polar than EtOH, k_{CS}/k_{CR} tends to slightly decrease with polarity (R^2 ($\log(k_{CS}/k_{CR})$ vs $f_O(\varepsilon)$) = 0.16). The media polarity, indeed, affects the Franck−Condon components of ET kinetics via the outer reorganization energy and via the driving force (eq 1), i.e., via the polarity dependence of reduction potentials, of W, and sometimes of $\mathcal{E}_{00}$ (for light sensitizers exhibiting solvatochromism). The scattered nature of the plots showing the polarity dependence of the CT kinetics and the moderate to weak correlations, however, indicate that other characteristics of the solvent media also govern the rates of CS and CR and especially the ratio between them, k_{CS}/k_{CR}.

Considering the solvent viscosity μ reveals additional trends. Both k_{CS} and k_{CR} tend to decrease with an increase in media viscosity (Figure 4d,e and Table 2). For CS, the media viscosity causes a distinct decrease in the rates only for relatively non-viscous solvents, i.e., for $\mu \leq 1$ mPa s (Figure 4d). An increase in media viscosity beyond 1 mPa s does not have a strong effect on k_{CS}, i.e., $R^2 \approx 0.05$ (Figure 4d). In addition to this weak correlation for media with $\mu \geq 1$ mPa, predominantly the polarity rather than the viscosity appears to affect CS. For the relatively viscous solvents, the polar ones (EG and DMSO) manifest noticeably higher k_{CS} than those of the relatively nonpolar ones (OctOH, BuOH, and EtOH) (Figure 4d).

Conversely, an increase in media viscosity impedes CR only for relatively viscous solvents, i.e., with $\mu \geq 1$ mPa s (Figure 4e). For nonvicious media, i.e., with $\mu \leq 1$ mPa s, the correlation between k_{CR} and μ is practically negligible (Figure 4e). This difference in the dependence of CS and CR on the media

Table 2. Kinetics of CS and CR of DPP-Ph for Solvents with Different Polarities and Viscosities[a]

solvent[b]	ε[c]	f_O[d]	μ (mPa s)[e]	$k_{CS} \times 10^{-10}$ (s^{-1})	$k_{CR} \times 10^{-10}$ (s^{-1})	k_{CS}/k_{CR}
1. DMSO	47.0	0.968	1.996	17.2 ± 1.1	5.09 ± 0.21	3.38 ± 0.35
2. EG	41.4	0.965	16.1	15.1 ± 3.9	1.44 ± 0.37	10.5 ± 5.4
3. MeCN	37.5	0.961	0.347	34.4 ± 1.2	4.63 ± 0.04	7.42 ± 0.33
4. MeOH	32.7	0.955	0.544	15.1 ± 3.0	6.48 ± 0.78	2.33 ± 0.75
5. EtOH	24.5	0.940	1.074	6.60 ± 1.74	4.05 ± 0.66	1.63 ± 0.70
6. *n*-BuOH	17.8	0.918	1.399	5.91 ± 0.48	1.18 ± 0.03	4.99 ± 0.55
7. OctOH	10.3	0.861	7.36	5.23 ± 1.39	0.741 ± 0.054	7.06 ± 2.40
8. DCM	8.93	0.841	0.410	16.9 ± 1.2	0.515 ± 0.006	32.7 ± 2.7
9. THF	7.58	0.814	0.481	20.9 ± 6.6	7.93 ± 1.28	2.63 ± 1.26
10. $CHCl_3$	4.81	0.718	0.536	8.12 ± 0.22	0.894 ± 0.010	9.08 ± 0.35

[a]The CS and CR rate constants, k_{CS} and k_{CR}, are obtained from global fits of **DPP-Ph** TA kinetics (see Supporting Information). [b]Solvents: dimethyl sulfoxide (DMSO), ethylene glycol (EG), acetonitrile (MeCN), methanol (MeOH), ethanol (EtOH), 1-butanol (BuOH), 1-octanol (OctOH), dichloromethane (DCM), tetrahydrofuran (THF), and chloroform ($CHCl_3$). [c]Static dielectric constant, i.e., relative permittivity. [d]Onsager function for solvent polarity, $f_O(\varepsilon) = 2(\varepsilon - 1)/(2\varepsilon + 1)$. [e]Dynamic viscosity.

DOI: 10.1021/jacs.6b04974
J. Am. Chem. Soc. 2016, 138, 12826−12832

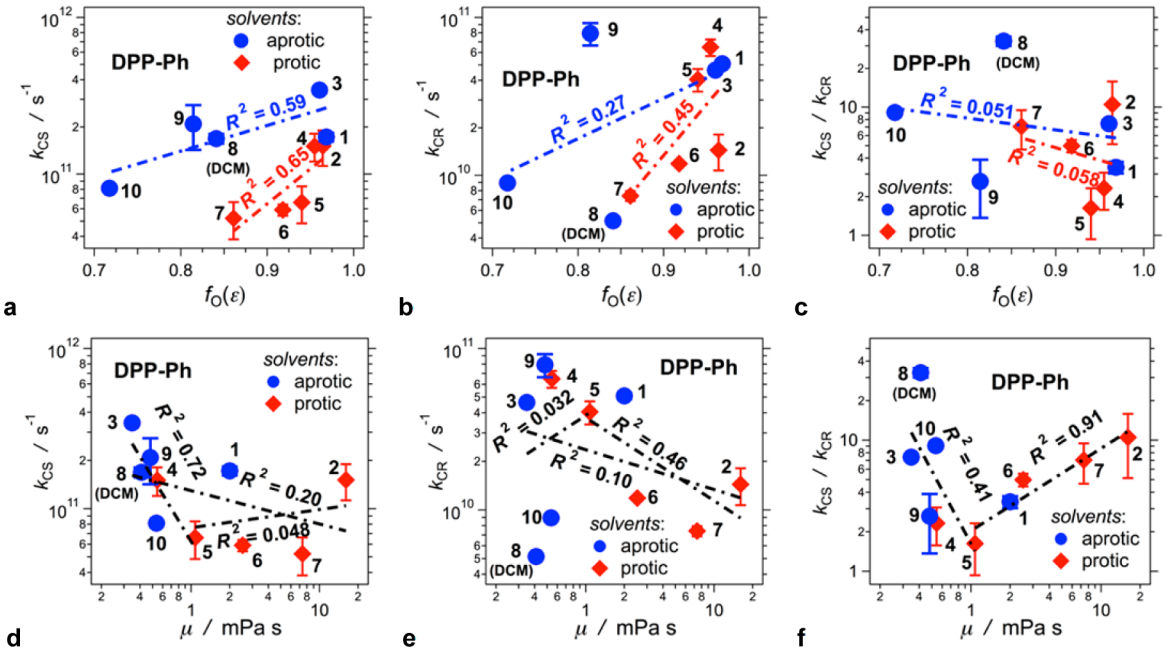

Figure 4. Solvent dependence of the rate constants of the photoinduced intramolecular charge separation, k_{CS}, and charge recombination, k_{CR}, of **DPP-Ph** (Table 2). (Solvents: 1 = DMSO, 2 = EG, 3 = MeCN, 4 = MeOH, 5 = EtOH, 6 = BuOH, 7 = OctOH, 8 = DCM, 9 = THF, and 10 = $CHCl_3$). The values of the rate constants are from global-fit analysis (see Supporting Information). (a–c) Dependence of k_{CS}, k_{CR}, and the ratio k_{CS}/k_{CR} on the media polarity, represented by the Onsager function for solvent polarity, $f_O(\varepsilon)$ (Table 2), with results from correlation analyses for protic (2, 4, 5, 6, and 7) and aprotic (1, 3, 8, 9, and 10) solvents. (d–f) Dependence of k_{CS}, k_{CR}, and the ratio k_{CS}/k_{CR} on the media viscosity, represented by the solvent dynamic viscosity, μ (Table 2), with results from correlation analyses: (d) for all solvents (R^2 = 0.20), for low-viscosity solvents with $\mu \leq 1$ mPa s (R^2 = 0.72), and for viscous solvents with $\mu \geq 1$ mPa s (R^2 = 0.048); (e) for all solvents (R^2 = 0.10), for low-viscosity solvents with $\mu \leq 1$ mPa s (R^2 = 0.032), and for viscous solvents with $\mu \geq 1$ mPa s (R^2 = 0. 46); and (f) for low-viscosity solvents with $\mu \leq 1$ mPa s (R^2 = 0.41) and for viscous solvents with $\mu \geq 1$ mPa s (R^2 = 0.91).

viscosity results in a bimodal effect of μ on k_{CS}/k_{CR} (Figure 4f). Indeed, the ratio k_{CS}/k_{CR} shows a well-defined dual dependence on the viscosity. The smallest k_{CS}/k_{CR} is that for ethanol (μ = 1.1 mPa s). Both a decrease and an increase in the solvent viscosity cause an increase in k_{CS}/k_{CR} (Figure 4f).

Rigidity of the environment, governed by the solvent viscosity, affects the frequency of molecular motions. Stretching, bending, and rotation around the N–C bond linking the donor with the acceptor are modes that can influence the kinetics of ET in **DPP-Ph**. While an increase in solvent viscosity may damp mostly low-frequency molecular vibrations, it also slows down the rotations around the N–C bond.

For systems such as **DPP-Ph**, in which a single covalent bond directly links a planar donor and acceptor, usually non-Condon, i.e., torsional, modes dominate the suppression of CR for nonviscous media. As observed for molecular rotors and particularly for those with propensity to form twisted intramolecular charge-transfer (TICT) states,[42] photoexcitation induces CS in states with a certain level of planarity and good electronic coupling between the π-conjugated systems of the donor and the acceptor. The formed CT sates exhibit a preference for conformers with orthogonality between the rings of the donor and the acceptor. Fast torsional modes produce these TICT states with decreased donor–acceptor electronic coupling and suppressed CR. As expected for molecular rotors, an increase in solvent viscosity impedes the fast torsional modes[43] that can compete with CR.

The excited-state behavior of **DPP-Ph** deviates from what would be expected for donor–acceptor dyads with propensity to form TICT excited states. Similar to TICT-forming conjugates, k_{CS}/k_{CR} for **DPP-Ph** decreases with an increase in media viscosity (for $\mu \leq 1$ mPa s, Figure 4f). While for TICT-forming conjugates a decrease in media viscosity leads to suppression of CR due to fast torsional modes, we cannot quite claim the same for **DPP-Ph**. Indeed, for solvents with $\mu \leq 1$ mPa s, an increase in μ tends to cause an increase in k_{CR} (Figure 4e), which appears consistent with the formation of a TICT excited state. The weak correlation between k_{CR} and μ, i.e., $R^2 < 0.05$ (Figure 4e), however, places a question on the significance of this trend for **DPP-Ph**. Conversely, the strong correlation (R^2 = 0.72) between k_{CS} and μ for **DPP-Ph** in relatively nonviscous solvents (Figure 4d) suggests that it is CS rather than CR that the media viscosity predominantly affects for $\mu \leq 1$ mPa s. That is, the distinct decrease in k_{CS} with an increase in viscosity (for $\mu \leq 1$ mPa s, Figure 4d) is the dominating effect responsible for the observed k_{CS}/k_{CR} versus μ trends (Figure 4f). This viscosity-induced suppression of CS suggests for solvent-coupled structural alterations of the locally excited state ^{1}**DPP*-Ph** that are essential for attaining fast ET rates. While faster than CR, the dynamics of nonviscous solvents is comparable with the picosecond time scales of CS (Table 2).

What appears quite unusual for DPP-Ph, however, is the suppression of CR and the increase in k_{CS}/k_{CR} by further increase in solvent viscosity, i.e., beyond 1 mPa s (Figure 4e,f). This trend is contrary to the expected behavior of TICT-forming donor–acceptor conjugates. While non-Condon modes can be behind the low-viscosity trends, they cannot account for the correlations observed for viscous media (Figure 4e,f). Furthermore, for all solvents except EG, the TA decays of the CT state, representing CR, are monoexponential, indicating that the time constants of CR significantly exceed the time scales of the involved structural dynamic modes.

DOI: 10.1021/jacs.6b04974
J. Am. Chem. Soc. 2016, 138, 12826–12832

A potential reason for this viscosity-induced decrease in k_{CR} and increase in k_{CS}/k_{CR} (for $\mu > 1$ mPa s) can be a suppression of vibrational and bending modes that are more important for CR than for CS. For example, fast vibrational modes that are not significantly affected by the solvent viscosity could dominate the Franck–Condon contribution to the rate constant of the transition from the locally excited to the CT state, i.e., CS: ^{1}**DPP***-**Ph** → **DPP**$^{\bullet-}$-**Ph**$^{\bullet+}$. Conversely, the transition from the CT to the ground state, i.e., CR: **DPP**$^{\bullet-}$-**Ph**$^{\bullet+}$ → **DPP-Ph**, may involve relatively slow vibrational modes that are susceptible to suppression by increased media viscosity.[44,45] The driving forces for CS are much smaller than those for CR. Hence, similar Frank–Codon effects on the ET kinetics most likely would affect CS more significantly than CR, which is opposite of the observed trends (Figure 4d,e). Therefore, the modes that govern CS should be quite different from those that are responsible for CR in order to attain the observed kinetic trends.

The dynamics of solvent reorganization may present another plausible contribution to the observed viscosity dependence trends (Figure 4d–f).[46−48] Despite the favorable thermodynamics, an increase in the viscosity slows down the dynamics of solvent response that can make it rate limiting for ET. This behavior would be expected for viscous polar solvents, such as EG. It appears, however, that the viscosity affects CS only for media with $\mu \leq 1$ mPa (Figure 4d). In addition, the similar values of k_{CS} for the two most polar alcohols, EG and MeOH, that have drastically different viscosities (Figure 4d and Table 2) place a question about the contribution of viscosity-limiting reorganization dynamics to the observed CS kinetics. Furthermore, the increase in k_{CS}/k_{CR} with the increase in solvent viscosity beyond 1 mPa s suggests that if such solvent reorganization dynamics plays a role in the observed kinetics it should affect the CR more than the CS processes. Such a discriminative impact on the CR rather than CS kinetics requires a significant difference between the polarity of the ground and the locally excited states. The solvent reorganization dynamics, hence, cannot provide a solid rationale for the observed suppression of CR as the viscosity increases beyond 1 mPa s.

When two saturated covalent bonds link the donor and the acceptor, as in **DPP-m-Ph**, the singlet-excited state of **DPP** is still significantly quenched (Figures 1b and 5a,b). The lifetime of ^{1}**DPP***-**m-Ph** is between 0.2 and 1 ns for the different solvents, i.e., 10–40 times smaller than that of ^{1}**DPP***. While the fluorescence lifetime of **DPP** shows no solvent dependence, the rates of decay of ^{1}**DPP***-**m-Ph** increase with an increase in the media polarity for solvents with $\varepsilon > 15$ (Figure 5c), which is consistent with photoinduced CS.

A transient absorption band at 640 nm, corresponding to **DPP**$^{\bullet-}$, appears along with the band of ^{1}**DPP*** upon the excitation of **DPP-m-Ph**. We, however, do not observe growth of **DPP**$^{\bullet-}$ as ^{1}**DPP*** decays (Figures 3c and 5c). In addition, the 640 nm transient absorption is less pronounced for less polar solvents, appearing mostly as a shoulder.

The flexibility of the methylene linker promotes heterogeneous CT kinetics representative of the multiple possible conformations of **DPP-m-Ph** with different donor–acceptor coupling. As a result, we observe CS and formation of **DPP**$^{\bullet-}$ within the excitation of **DPP-m-Ph**, as well as biexponential decays for some of the solvent media.

These findings suggest that while ^{1}**DPP***-**m-Ph** undergoes efficient CS, the consecutive CR occurs with comparable or faster rates. That is, CS is the rate-limiting step, and the competing CR is fast enough to prevent accumulation of the CT state, except

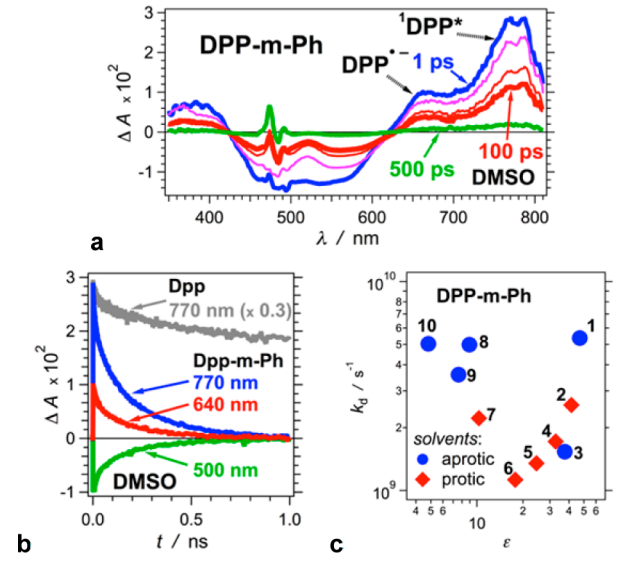

Figure 5. Transient absorption (TA) dynamics of **DPP-m-Ph**. (a) TA spectra for DMSO (λ_{ex} = 480 nm, 6 μJ per pulse, fwhm$_{(for\ 800\ nm)}$ = 50 fs). (b) TA dynamics monitored at different wavelengths: 770 nm for ^{1}**DPP***, 640 nm for **DPP**$^{\bullet-}$, and 500 nm for ground-state bleach recovery. For comparison, the top gray line is for **DPP** monitored at 770 nm (Figure 3a). The rest of the kinetic curves are for **DPP-m-Ph**. (c) Dependence of the decay rate constant, k_d, recorded at 770 nm, on the solvent polarity represented by the solvent static relative dielectric constant, ε. The solvent numeration is the same as that in both Table 2 and Figure 4.

when CS occurs within the duration of the femtosecond excitation pulse. Indeed, the appearance of both **DPP**$^{\bullet-}$ and ^{1}**DPP*** transients within the femtosecond excitation pulse, while ^{1}**DPP*** lives hundreds of picoseconds, suggests for multiple CS pathways. The flexible methylene linker permits access to conformers where the donor contacts directly one of the trifluoromethylphenyl moieties, providing pathways for ultrafast CS. Folded conformers with improved donor–acceptor coupling dominating the locally excited states in nonpolar media can explain the relatively large decay constants for solvents with $\varepsilon < 15$ (Figure 5c).

Along with the conformational heterogeneity, in comparison with **DPP-Ph**, an increase in the inner reorganizational energy for **DPP-m-Ph** can push the tips of the Marcus curves closer to the CR and away from the CS rates, making $k_{CS} < k_{CR}$. Overall the findings for the excited-state dynamics of **DPP-m-Ph** reveal a key advantage in the molecular-rotor design of **DPP-Ph** for suppressing the undesired CR.

CONCLUSIONS

While $\Delta G^{(0)}_{CS}$ and $\Delta G^{(0)}_{CR}$ are similar for both dyads, $k_{CS} > k_{CR}$ for **DPP-Ph**, whereas $k_{CS} \leq k_{CR}$ for **DPP-m-Ph**. This feature reiterates the importance of the molecular-rotor design of the **DPP-Ph** dyad for impeding CR while attaining efficient CS. Suppressing CR and boosting CS in nonviscous solvents can indeed be in accordance with expected non-Condon effects. The viscosity-induced increase in the difference between the rates of CS and CR, however, suggests for dominating synergy with vibronic modes and, perhaps, solvent reorganizational dynamics. Impeding CR, while conserving the efficiency of CS, is key for organic electronic materials and devices where molecular confinement can govern their properties. The findings for viscous media provide a potential platform for translation of molecular designs to solid-state applications.

DOI: 10.1021/jacs.6b04974
J. Am. Chem. Soc. 2016, 138, 12826–12832

■ ASSOCIATED CONTENT

Supporting Information

The Supporting Information is available free of charge on the ACS Publications website at DOI: 10.1021/jacs.6b04974.

Experimental details for the synthesis and characterization of the final compounds and the key intermediates and for the electrochemical and spectroscopic experiments (PDF)

■ AUTHOR INFORMATION

Corresponding Authors

*dtgryko@icho.edu.pl

*vullev@ucr.edu

Present Address

J.J.R.: Instituto de Investigaciones Fisicoquímicas Teóricas y Aplicadas (INIFTA), Facultad de Ciencias Exactas, Universidad Nacional de La Plata, Casilla de Correo 16, Sucursal 4, 1900 La Plata, Argentina.

Author Contributions

A.P. and E.M.E. contributed equally to this work.

Notes

The authors declare no competing financial interest.

■ ACKNOWLEDGMENTS

This work is supported by the Polish National Science Centre, grants MAESTRO-2012/06/A/ST5/00216, and PRELUDIUM UMO-2013/09/N/ST5/02974, Foundation for Polish Science START programme, and the U.S.A. National Science Foundation, grants CHE 1465284 and CBET 0923408. J.J.R. was supported by Consejo Nacional de Investigaciones Científicas y Técnicas (CONICET), Argentina (Ph.D. fellowship) and bec.ar - Fulbright Comission (exchange fellowships).

■ REFERENCES

(1) Bao, D.; Upadhyayula, S.; Larsen, J. M.; Xia, B.; Georgieva, B.; Nunez, V.; Espinoza, E. M.; Hartman, J. D.; Wurch, M.; Chang, A.; Lin, C.-K.; Larkin, J.; Vasquez, K.; Beran, G. J. O.; Vullev, V. I. *J. Am. Chem. Soc.* **2014**, *136*, 12966−12973.

(2) Savoie, B. M.; Rao, A.; Bakulin, A. A.; Gelinas, S.; Movaghar, B.; Friend, R. H.; Marks, T. J.; Ratner, M. A. *J. Am. Chem. Soc.* **2014**, *136*, 2876−2884.

(3) Gust, D.; Moore, T. A.; Moore, A. L.; Lee, S. J.; Bittersmann, E.; Luttrull, D. K.; Rehms, A. A.; DeGraziano, J. M.; Ma, X. C.; Gao, F.; Belford, R. E.; Trier, T. T. *Science* **1990**, *248*, 199−201.

(4) Jones, G., II; Vullev, V.; Braswell, E. H.; Zhu, D. *J. Am. Chem. Soc.* **2000**, *122*, 388−389.

(5) Whitesell, J. K.; Chang, H. K.; Fox, M. A.; Galoppini, E.; Watkins, D. M.; Fox, H.; Hong, B. *Pure Appl. Chem.* **1996**, *68*, 1469−1474.

(6) Jones, G., II; Vullev, V. I. *Org. Lett.* **2002**, *4*, 4001−4004.

(7) Marcus, R. A.; Sutin, N. *Biochim. Biophys. Acta, Rev. Bioenerg.* **1985**, *811*, 265−322.

(8) Thomas, K. G.; George, M. V.; Kamat, P. V. *Helv. Chim. Acta* **2005**, *88*, 1291−1308.

(9) Rosspeintner, A.; Angulo, G.; Vauthey, E. *J. Am. Chem. Soc.* **2014**, *136*, 2026−2032.

(10) Lainé, P. P.; Campagna, S.; Loiseau, F. *Coord. Chem. Rev.* **2008**, *252*, 2552−2571.

(11) Jang, S.; Newton, M. D. *J. Chem. Phys.* **2005**, *122*, 024501.

(12) Berlin, Y. A.; Grozema, F. C.; Siebbeles, L. D. A.; Ratner, M. A. *J. Phys. Chem. C* **2008**, *112*, 10988−11000.

(13) Grzybowski, M.; Gryko, D. T. *Adv. Opt. Mater.* **2015**, *3*, 280−320.

(14) Iqbal, A.; Jost, M.; Kirchmayr, R.; Pfenninger, J.; Rochat, A.; Wallquist, O. *Bull. Soc. Chim. Belg.* **1988**, *97*, 615−643.

(15) Qu, S.; Tian, H. *Chem. Commun.* **2012**, *48*, 3039−3051.

(16) Nielsen, C. B.; Turbiez, M.; McCulloch, I. *Adv. Mater.* **2013**, *25*, 1859−1880.

(17) Grzybowski, M.; Glodkowska-Mrowka, E.; Stoklosa, T.; Gryko, D. T. *Org. Lett.* **2012**, *14*, 2670−2673.

(18) Kaur, M.; Choi, D. H. *Chem. Soc. Rev.* **2015**, *44*, 58−77.

(19) Ftouni, H.; Bolze, F.; de Rocquigny, H.; Nicoud, J. F. *Bioconjugate Chem.* **2013**, *24*, 942−950.

(20) Shimizu, S.; Iino, T.; Araki, Y.; Kobayashi, N. *Chem. Commun.* **2013**, *49*, 1621−1623.

(21) Fischer, G. M.; Ehlers, A. R.; Zumbusch, A.; Daltrozzo, E. *Angew. Chem., Int. Ed.* **2007**, *46*, 3750−3753.

(22) Yue, W.; Suraru, S.-L.; Bialas, D.; Müller, M.; Würthner, F. *Angew. Chem., Int. Ed.* **2014**, *53*, 6159−6162.

(23) Morton, C. J. H.; Gilmour, R.; Smith, D. M.; Lightfoot, P.; Slawin, A. M. Z.; MacLean, E. J. *Tetrahedron* **2002**, *58*, 5547−5565.

(24) Morton, C. J. H.; Riggs, R. L.; Smith, D. M.; Westwood, N. J.; Lightfoot, P.; Slawin, A. M. Z. *Tetrahedron* **2005**, *61*, 727−738.

(25) Riggs, R. L.; Morton, C. J. H.; Slawin, A. M. Z.; Smith, D. M.; Westwood, N. J.; Austen, W. S. D.; Stuart, K. E. *Tetrahedron* **2005**, *61*, 11230−11243.

(26) Guo, S.; Bao, D.; Upadhyayula, S.; Wang, W.; Guvenc, A. B.; Kyle, J. R.; Hosseinibay, H.; Bozhilov, K. N.; Vullev, V. I.; Ozkan, C. S.; Ozkan, M. *Adv. Funct. Mater.* **2013**, *23*, 5199−5211.

(27) Vullev, V. I.; Jones, G. *Tetrahedron Lett.* **2002**, *43*, 8611−8615.

(28) Bao, D.; Millare, B.; Xia, W.; Steyer, B. G.; Gerasimenko, A. A.; Ferreira, A.; Contreras, A.; Vullev, V. I. *J. Phys. Chem. A* **2009**, *113*, 1259−1267.

(29) Bao, D.; Ramu, S.; Contreras, A.; Upadhyayula, S.; Vasquez, J. M.; Beran, G.; Vullev, V. I. *J. Phys. Chem. B* **2010**, *114*, 14467−14479.

(30) Larsen, J. M.; Espinoza, E. M.; Hartman, J. D.; Lin, C.-K.; Wurch, M.; Maheshwari, P.; Kaushal, R. K.; Marsella, M. J.; Beran, G. J. O.; Vullev, V. I. *Pure Appl. Chem.* **2015**, *87*, 779−792.

(31) Espinoza, E. M.; Larsen, J. M.; Vullev, V. I. *J. Phys. Chem. Lett.* **2016**, *7*, 758−764.

(32) Espinoza, E. M.; Xia, B.; Darabedian, N.; Larsen, J. M.; Nunez, V.; Bao, D.; Mac, J. T.; Botero, F.; Wurch, M.; Zhou, F.; Vullev, V. I. *Eur. J. Org. Chem.* **2016**, *2016*, 343−356.

(33) Wan, J.; Ferreira, A.; Xia, W.; Chow, C. H.; Takechi, K.; Kamat, P. V.; Jones, G.; Vullev, V. I. *J. Photochem. Photobiol., A* **2008**, *197*, 364−374.

(34) Flamigni, L.; Ventura, B.; Tasior, M.; Becherer, T.; Langhals, H.; Gryko, D. T. *Chem. - Eur. J.* **2008**, *14*, 169−183.

(35) Jones, G., II; Yan, D.; Hu, J.; Wan, J.; Xia, B.; Vullev, V. I. *J. Phys. Chem. B* **2007**, *111*, 6921−6929.

(36) Hu, J.; Xia, B.; Bao, D.; Ferreira, A.; Wan, J.; Jones, G.; Vullev, V. I. *J. Phys. Chem. A* **2009**, *113*, 3096−3107.

(37) Jin, R. *Theor. Chem. Acc.* **2012**, *131*, 1260.

(38) Shi, H.; Sun, W.; Wang, Q.; Gu, G.; Si, W.; Huang, W.; Zhang, Q.; Dong, X. *ChemPlusChem* **2016**, *81*, 515−520.

(39) Rehm, D.; Weller, A. *Isr. J. Chem.* **1970**, *8*, 259.

(40) Xia, B.; Bao, D.; Upadhyayula, S.; Jones, G.; Vullev, V. I. *J. Org. Chem.* **2013**, *78*, 1994−2004.

(41) Upadhyayula, S.; Bao, D.; Millare, B.; Sylvia, S. S.; Habib, K. M. M.; Ashraf, K.; Ferreira, A.; Bishop, S.; Bonderer, R.; Baqai, S.; Jing, X.; Penchev, M.; Ozkan, M.; Ozkan, C. S.; Lake, R. K.; Vullev, V. I. *J. Phys. Chem. B* **2011**, *115*, 9473−9490.

(42) Sasaki, S.; Drummen, G. P. C.; Konishi, G.-i. *J. Mater. Chem. C* **2016**, *4*, 2731−2743.

(43) Zhou, F.; Shao, J.; Yang, Y.; Zhao, J.; Guo, H.; Li, X.; Ji, S.; Zhang, Z. *Eur. J. Org. Chem.* **2011**, 4773−4787.

(44) Bagchi, B.; Biswas, R. *Adv. Chem. Phys.* **1999**, *109*, 207−433.

(45) Sokoloff, J. B. *J. Chem. Phys.* **1988**, *89*, 2330−2335.

(46) Clark, C. D.; Hoffman, M. Z. *Coord. Chem. Rev.* **1997**, *159*, 359−373.

(47) Canzi, G.; Kubiak, C. P. *J. Phys. Chem. C* **2012**, *116*, 6560−6566.

(48) Chakrabarti, S.; Liu, M.; Waldeck, D. H.; Oliver, A. M.; Paddon-Row, M. N. *J. Phys. Chem. A* **2009**, *113*, 1040−1048.

DOI: 10.1021/jacs.6b04974
J. Am. Chem. Soc. 2016, 138, 12826−12832